Vector Current Control Derived from Direct Power Control for Grid-Connected Inverters

Gui, Yonghao; Wang, Xiongfei; Blaabjerg, Frede

Published in:
I E E E Transactions on Power Electronics

DOI (link to publication from Publisher):
10.1109/TPEL.2018.2883507

Publication date:
2019

Document Version
Accepted author manuscript, peer reviewed version

Vector Current Control Derived from Direct Power Control for Grid-Connected Inverters

Yonghao Gui, *Member, IEEE*, Xiongfei Wang, *Senior Member, IEEE* and Frede Blaabjerg, *Fellow, IEEE*

***Abstract*—We propose a vector current control derived from direct power control (VCC-DPC) for a three-phase voltage source inverter (VSI) in the synchronous rotating frame through instantaneous real and reactive powers. The proposed VCC-DPC method has the same control structure as the conventional VCC except for the coordinate transformation, since we obtain the d–q axes currents model of VSI without using Park transformation and the PLL system. Consequently, the proposed method has the same property as the conventional VCC if the PLL extracts the phase angle of the grid voltage correctly. However, with the consideration of the slow dynamics of the PLL, the proposed method has an enhanced dynamical performance feature compared with the conventional VCC. Moreover, it has another benefit that the reduction of the computational burden could be expected since there is no Park transformation and the PLL in the controller implementation. We can guarantee that the closed-loop system with the proposed method is exponentially stable in the operating range. Finally, both simulation and experimental results using a 15-kW-inverter system match the theoretical expectations closely.**

***Index Terms*—Voltage source inverter, vector current controller, instantaneous real and reactive powers, exponentially stable.**

I. Introduction

POWER converters are widely used in the application of renewable energy sources and distributed generation systems [1]–[4]. One of the key devices of power converters is grid-connected voltage source inverter (VSI), which is used to transform the DC power to AC power. Recently, various control strategies have been developed to improve its reliability, efficiency, and safety by engineers and researchers [5]–[10].

A standard control strategy of grid-connected VSI is vector current control (VCC), which is designed in a synchronous rotating reference frame. The main advantage is that it transforms the AC values to the DC ones by using coordinate transformation and thus the linear PI controller can be used to indirectly control real and reactive powers by controlling *d*–*q* axes currents separately [11]. Moreover, the dynamics of VSI is changed into a linear time-invariant (LTI) system in the synchronous rotating reference frame. By means of this, the VSI system can be easily designed and analyzed by using the linear control techniques [12]–[18]. For the standard VCC, since the *d*–*q* axes currents have to be in phase with the grid voltage, the phase angle used by the Park transformation has to be extracted from the grid voltages correctly [1]. One possible method to extract the phase angle is filtering of the grid voltages and using arctangent function [19]–[21]. Nowadays, a phase-locked loop (PLL) is a more common method to extract the phase angle of the grid voltage for VSIs [22], [23]. However, the PLL system will cause a slow transient response. In addition, it may cause the instability problem in some cases [24]–[30].

Another control method, direct power control (DPC) has been researched for VSIs to control instantaneous real and reactive powers directly without using any inner-loop current regulator [31], [32]. However, these methods have a variable switching frequency according to the switching state, which will cause an unexpected broadband harmonic spectrum range, *i.e.* it is not easy to design a line filter. To achieve a constant switching frequency, some other DPC algorithms have been proposed by using space vector modulation [32], [33], or calculating required converter voltage vector in each switching period [34], [35]. Moreover, for the robust property, a sliding mode control based DPC is designed to obtain an exponential convergence of the tracking error of the real and reactive powers [36], and a passivity-based control DPC is designed by considering the system's intrinsic dissipative nature [37]. However, there are still power ripples in both real and reactive powers. Another optimal control strategy, model predictive control (MPC)-DPC, has been proposed by considering the multivariable case, system constraints, and nonlinearities in an intuitive way [38]–[43]. MPC-DPC selects voltage vector sequence and calculates duty cycles in every sampling period. One of the advantages is that it provides a constant switching frequency. However, it may incur additional computational burden. In addition, *Cheng and Nian* proposed a virtual synchronous reference frame based DPC for VSI in [44] and extended it to doubly fed induction generator system with consideration of unbalance grid voltage and harmonically distorted voltage conditions [45], [46]. They used a virtual phase angle instead of the voltage phase angle acquired by PLL for coordinate transformations, and apply the reduced-order vector integrators to directly regulate the power pulsations.

Recently, *Gui et al.* introduced a grid voltage modulated-DPC (GVM-DPC), which has a good transient response and steady-state performance [47]–[49]. The key point of the GVM-DPC is that converts the original nonlinear system into an LTI system, which also can be easily designed and analyzed by using various linear control techniques [50].

In this paper, we propose a vector current control derived from direct power control (VCC-DPC) for the three-phase

This work was supported by the REliable Power Electronic-Based Power System (REPEPS) project at the Department of Energy Technology, Aalborg University as a part of the Villum Investigator Program funded by the Villum Foundation. *(Corresponding Author: Xiongfei Wang.)*

The authors are with the Department of Energy Technology, Aalborg University, 9220 Aalborg, Denmark. (e-mail: yog@et.aau.dk; xwa@et.aau.dk; fbl@et.aau.dk).

VSI. The proposed method should have the same property as the conventional VCC, since we get the d–q axes currents model of the VSI through the DPC model. However, due to the absence of Park transformation and PLL, the proposed method has enhanced performance in the case considering the slow dynamics of PLL, and the reduction of the computational burden could be expected in comparison with the conventional VCC. We found that our concept is similar to the methods designed in [19], [20], [51], [52]. However, the proposed method combines the advantages of DPC and standard VCC, since it starts from the DPC model. Moreover, it can directly control the current to obtain a high quality performance which is a general requirement in the industry. In this paper, we design a simple controller with a feedforward and feedback structure to compare the performance with the conventional VCC fairly. However, various controllers could be designed based on the proposed technique to improve the performance or resolve some practical issues. The main contribution of the paper is that the proposed control method synchronizes the VSI to the grid through the direct power calculation method instead of the PLL system. If the grid voltage is distorted and imbalanced, then both the proposed method and conventional approaches will need additional digital filters. However, the performance of the proposed method is not affected by the PLL system, which may not estimate the correct phase angle of the grid voltage during the transient or even destabilizes the system in a weak grid [8], [53], [54]. In summary, we can expect the following features as follows:

- The proposed method could stabilize the weak-grid-connected VSI system.
- The proposed method has a good fault ride through (FRT) performance.
- The proposed method is robust to the parameter uncertainties (*e.g.* line filter and grid frequency, etc.).

Finally, both simulation and experimental results match the theoretical expectations closely.

The rest of the paper is organized as follows. Section II presents the system modeling of the grid-connected VSI based on the DPC model. In Section III, we design a simple controller with a feedforward and feedback structure. Section IV shows the simulation results using MATLAB/Simulink, Simscape Power Systems. In Section V, we also validate the proposed technique via the experimental test using a 15-kW-inverter system. Finally, Section VI gives the conclusions of this work.

II. Modeling of Voltage Source Inverters

In this Section, at first, a DPC modeling of VSC is briefly introduced. Then, the GVM-DPC is introduced for the VSC system to make it be an LTI system.

Fig. 1 shows a two-level VSI connected to the grid through an L-filter. In this study, we assume that a stiff DC source is connected to the DC-side of the inverter, *e.g.*, a rectifier in wind application or a DC-DC converter in PV application. Consequently, the dynamics from the DC input is not studied in this paper. The dynamic equations consisting of the output

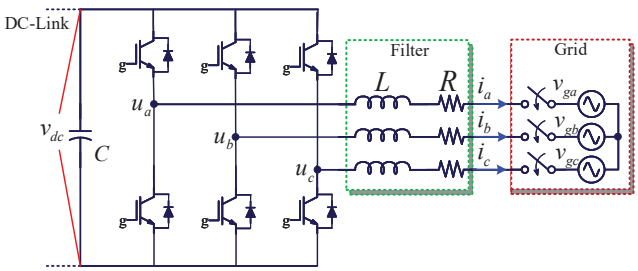

Fig. 1. Grid-connected voltage source inverter with an L filter.

voltages of the VSI, the grid voltages, and the output currents can be expressed as follows:

$$\begin{aligned} L\frac{di_a}{dt} &= -Ri_a + u_a - v_{ga}, \\ L\frac{di_b}{dt} &= -Ri_b + u_b - v_{gb}, \\ L\frac{di_c}{dt} &= -Ri_c + u_c - v_{gc}, \end{aligned} \tag{1}$$

where i_{abc}, v_{gabc}, u_{abc} are the output currents, the grid voltages, and the output voltages of the VSI in the abc frame, respectively. L and R are the filter inductance and resistance, respectively. Based on a balanced grid voltage condition, the dynamic equations in (1) can be transformed into the stationary reference frame by using Clark transformation as follows:

$$\begin{aligned} L\frac{di_\alpha}{dt} &= -Ri_\alpha + u_\alpha - v_{g\alpha}, \\ L\frac{di_\beta}{dt} &= -Ri_\beta + u_\beta - v_{g\beta}, \end{aligned} \tag{2}$$

where $i_{\alpha\beta}$, $v_{g\alpha\beta}$, and $u_{\alpha\beta}$ indicate the output currents, the grid voltages, and the VSC output voltages in the α–β frame.

Then, we can obtain the instantaneous real and reactive powers injected from VSI to the grid in the stationary reference frame as follows [55], [56]:

$$\begin{aligned} p &= \frac{3}{2}(v_{g\alpha}i_\alpha + v_{g\beta}i_\beta), \\ q &= \frac{3}{2}(v_{g\beta}i_\alpha - v_{g\alpha}i_\beta), \end{aligned} \tag{3}$$

where P and Q are the instantaneous real and reactive powers injected into the grid, respectively. To obtain the dynamic equation of the powers, we differentiate (3) with respect to time. Then, the instantaneous real and reactive power of dynamic equations are expressed as follows:

$$\begin{aligned} \frac{dp}{dt} &= \frac{3}{2}\left(i_\alpha\frac{dv_{g\alpha}}{dt} + v_{g\alpha}\frac{di_\alpha}{dt} + i_\beta\frac{dv_{g\beta}}{dt} + v_{g\beta}\frac{di_\beta}{dt}\right), \\ \frac{dq}{dt} &= \frac{3}{2}\left(i_\alpha\frac{dv_{g\beta}}{dt} + v_{g\beta}\frac{di_\alpha}{dt} - i_\beta\frac{dv_{g\alpha}}{dt} - v_{g\alpha}\frac{di_\beta}{dt}\right). \end{aligned} \tag{4}$$

Note that the powers dynamics in (4) consist of the grid voltages and output currents dynamics. To simplify the powers dynamics in (4), we consider a non-distorted grid in this study. Thus, the following relationship could be obtained such as

$$\begin{aligned} v_{g\alpha} &= V_g\cos(\omega t), \\ v_{g\beta} &= V_g\sin(\omega t), \end{aligned} \tag{5}$$

where

$$V_g = \sqrt{v_{g\alpha}^2 + v_{g\beta}^2}. \tag{6}$$

Note that, V_g is the magnitude of the grid voltage, ω is the angular frequency of the grid voltage and $\omega = 2\pi f$, and f is the frequency of the grid voltage. To obtain the instantaneous grid voltage dynamic equations, we differentiate (5) with respect to time as follows:

$$\begin{aligned} \frac{dv_{g\alpha}}{dt} &= -\omega V_g \sin(\omega t) = -\omega v_{g\beta}, \\ \frac{dv_{g\beta}}{dt} &= \omega V_g \cos(\omega t) = \omega v_{g\alpha}. \end{aligned} \tag{7}$$

Substituting (1) and (7) into (4), the dynamics of the real and reactive powers are represented as follows [36]:

$$\begin{aligned} \frac{dp}{dt} &= -\frac{R}{L}p - \omega q + \frac{3}{2L}(v_{g\alpha}u_\alpha + v_{g\beta}u_\beta - V_g^2), \\ \frac{dq}{dt} &= \omega p - \frac{R}{L}q + \frac{3}{2L}(v_{g\beta}u_\alpha - v_{g\alpha}u_\beta). \end{aligned} \tag{8}$$

Note that, the dynamics of instantaneous real and reactive powers in (8) are a multi-input-multi-output (MIMO) system, where u_α and u_β are the control inputs and p and q are the outputs. Moreover, the system is a time-varying one since both control inputs are multiplied by the grid voltages. To simplify the dynamics in (8), we use the GVM control inputs defined in [47], [48], which are a similar concept in [20], [51] as follows:

$$\begin{aligned} u_P &:= v_{g\alpha}u_\alpha + v_{g\beta}u_\beta, \\ u_Q &:= v_{g\beta}u_\alpha - v_{g\alpha}u_\beta, \end{aligned} \tag{9}$$

where u_P and u_Q are the new control inputs, which will be designed. Note that, u_P and u_Q are changed into DC components since they satisfy the following relationship based on the assumption of the non-distorted grid voltages in (5).

$$\begin{bmatrix} u_P \\ u_Q \end{bmatrix} = V_g \begin{bmatrix} \cos(\omega t) & \sin(\omega t) \\ \sin(\omega t) & -\cos(\omega t) \end{bmatrix} \begin{bmatrix} u_\alpha \\ u_\beta \end{bmatrix} = V_g \begin{bmatrix} u_d \\ -u_q \end{bmatrix}, \tag{10}$$

where u_d and u_q indicate the converter voltages in the d–q frame. Note that, the GVM method in (9) does not use the PLL, but the control inputs are represented in the d–q frame. With the new control inputs defined in (9), the dynamics of the real and reactive powers in (8) can be rewritten as follows:

$$\begin{aligned} \frac{dp}{dt} &= -\frac{R}{L}p - \omega q + \frac{3}{2L}(u_P - V_g^2), \\ \frac{dq}{dt} &= \omega p - \frac{R}{L}q + \frac{3}{2L}u_Q. \end{aligned} \tag{11}$$

Note that, the dynamics of the real and reactive powers in (11) is changed into a time-invariant MIMO system with the coupling states. In addition, the model in (11) has a similar structure as the model of d–q axes currents of VSI. Then, we will show the relationship between the model in (11) and the model of d–q axes currents for VSI.

In the synchronous frame, since the d-axis is always coincident with the instantaneous voltage vector and the q-axis is in quadrature with it, $v_{gd} = V_g$ and $v_{gq} = 0$, the real and reactive powers in the d–q frame can be defined as follows:

$$\begin{aligned} p &= \frac{3}{2}v_{gd}i_d, \\ q &= \frac{3}{2}v_{gd}i_q. \end{aligned} \tag{12}$$

If we multiply $\frac{2}{3V_g}$ to both side of the dynamics of the real and reactive powers in (11), the new system can be obtained as follows:

$$\begin{aligned} \frac{di_d}{dt} &= -\frac{R}{L}i_d - \omega i_q + \frac{1}{L}(u_d - V_g), \\ \frac{di_q}{dt} &= \omega i_d - \frac{R}{L}i_q + \frac{1}{L}u_q. \end{aligned} \tag{13}$$

Note that the proposed model in (13) is changed into a conventional currents model in the d–q frame, but the PLL system is not used for this method.

III. Controller Design

In this Section, a simple controller consisting of feedforward and feedback is designed for the new system in (13) to regulate the d–q axes currents. However, various controllers especially the linear ones could be designed based on the proposed technique (for the new system in (13)) to improve the performance or resolve some practical issues.

At first step, the errors of the d–q axes currents are defined as follows:

$$\begin{aligned} e_{i_d} &:= i_{dref} - i_d, \\ e_{i_q} &:= i_{qref} - i_q, \end{aligned} \tag{14}$$

where i_{dref} and i_{qref} are the references of the d–q axes currents, respectively. To cancel the coupling terms in (13), a controller consisting of feedforward and feedback terms is designed as follows:

$$\begin{aligned} u_d &= \underbrace{V_g + L\omega i_q}_{feedforward} + \underbrace{\nu_{i_d}}_{feedback}, \\ u_q &= \underbrace{L\omega i_d}_{feedforward} + \underbrace{\nu_{i_q}}_{feedback}, \end{aligned} \tag{15}$$

where ν_{i_d} and ν_{i_q} are the feedback control inputs. Note that, with the proposed controller in (15), the new feedback inputs, ν_{i_d} and ν_{i_q}, and the dynamics of real and reactive powers have a linear relationship. To obtain zero steady-state error, a PI controller is applied to ν_{i_d} and ν_{i_q} as follows:

$$\begin{aligned} \nu_{i_d} &= K_{i_d,p}e_{i_d} + K_{i_d,i}\int_0^t e_{i_d}(\tau)d\tau, \\ \nu_{i_q} &= K_{i_q,p}e_{i_q} + K_{i_q,i}\int_0^t e_{i_q}(\tau)d\tau, \end{aligned} \tag{16}$$

where $K_{i_d,p}$, $K_{i_d,i}$, $K_{i_q,p}$, and $K_{i_q,i}$ are the PI controller gains.

Consequently, substituting (15) and (16) into (13), the following error dynamics are obtained such as

$$\begin{aligned} \dot{e}_{i_d} &= -K_{i_d,p}e_{i_d} - K_{i_d,i}\int_0^t e_{i_d}(\tau)d\tau, \\ \dot{e}_{i_q} &= -K_{i_q,p}e_{i_q} - K_{i_q,i}\int_0^t e_{i_q}(\tau)d\tau. \end{aligned} \tag{17}$$

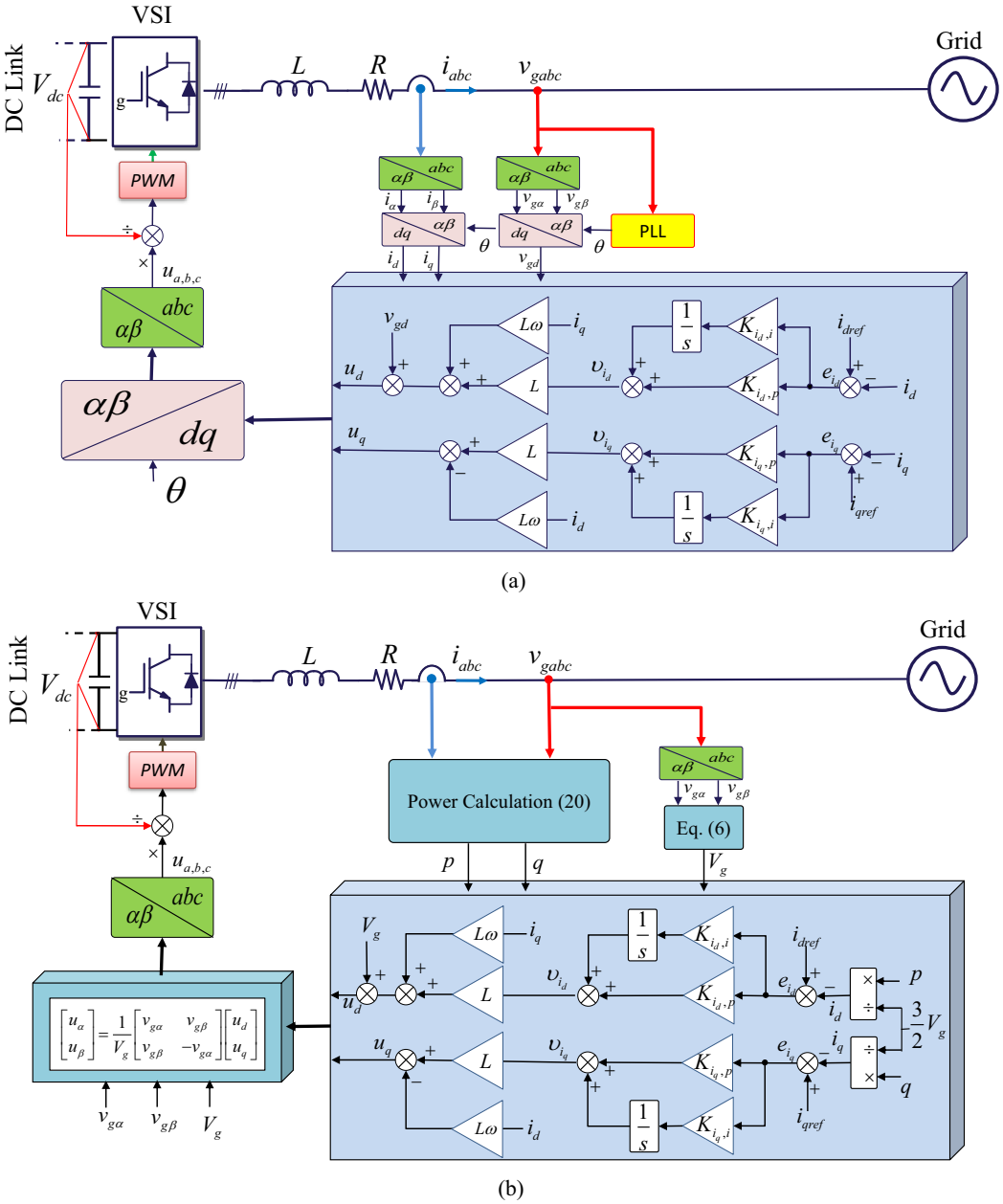

Fig. 2. Block diagram of (a) the standard VCC with PLL; (b) the proposed method without PLL.

Note that, if the PI controller gains are selected as positive values, then the closed-loop system is exponentially stable in the operating range. It can easily be proven by using the following equation. Defining $\dot{\psi}_{i_d} = e_{i_d}$ and $\dot{\psi}_{i_q} = e_{i_q}$, the error dynamics (17) can be represented as

$$\underbrace{\begin{bmatrix} \dot{e}_{i_d} \\ \dot{\psi}_{i_d} \\ \dot{e}_{i_q} \\ \dot{\psi}_{i_q} \end{bmatrix}}_{\dot{x}} = \underbrace{\begin{bmatrix} -K_{i_d,p} & -K_{i_d,i} & 0 & 0 \\ 1 & 0 & 0 & 0 \\ 0 & 0 & -K_{i_q,p} & -K_{i_q,i} \\ 0 & 0 & 1 & 0 \end{bmatrix}}_{A_{cl}} \underbrace{\begin{bmatrix} e_{i_d} \\ \psi_{i_d} \\ e_{i_q} \\ \psi_{i_q} \end{bmatrix}}_{x}, \tag{18}$$

where x is the state of the system, and A_{cl} is the state-space matrix of the closed-loop of the system. If $K_{i_d,p}$, $K_{i_d,i}$, $K_{i_q,p}$, and $K_{i_q,i}$ are positive values, then A has all negative eigenvalues.

Finally, the original control inputs u_α and u_β are calculated based on the inverse of (10) as follows:

$$\begin{aligned} u_\alpha &= \frac{v_{g\alpha} u_d + v_{g\beta} u_q}{V_g}, \\ u_\beta &= \frac{v_{g\beta} u_d - v_{g\alpha} u_q}{V_g}. \end{aligned} \tag{19}$$

The block diagrams of the conventional VCC and the proposed method are shown in Fig. 2. Instead of (3), we could use a set of three-phase voltages and currents to instantaneous real

TABLE I
SYSTEM PARAMETERS USED IN SIMULATIONS AND EXPERIMENTS

Parameter	Symbol	Value	Unit
Nominal Grid Voltage	$V_{ga,rms}$	110	V
Nominal Grid Frequency	f	50	Hz
DC-Link Voltage	V_{dc}	730	V
Filter Inductance	L	5	mH
Filter Resistance	R	0.15	Ω
Switching Frequency	f_{sw}	10	kHz

and reactive powers such as

$$p = v_{ga}i_a + v_{gb}i_b + v_{gc}i_c,$$
$$q = \frac{1}{\sqrt{3}}[(v_{gb} - v_{gc})i_a - (v_{gc} - v_{ga})i_b + (v_{ga} - v_{gb})i_c]. \quad (20)$$

Compared to the conventional VCC, there is no PLL, Park transformation, and inverse Park transformation in the implementation of the proposed method.

IV. SIMULATION RESULTS

To validate the proposed control method, we use MATLAB/Simulink, Simscape Power Systems. The parameters of the system used in the simulation are listed in Table I.

At first, we compare two methods when the reference of i_d is suddenly changed, as shown in Fig. 3. To compare i_d tracking performance from Fig. 3(b), the time response of the proposed method without the PLL and Park transformation is similar to that of the conventional VCC method since the PLL continually provide the correct information of θ. Moreover, the performance of i_q, P, and Q with both methods is similar as well. The second case is that the inverter is connected to the grid and injects power to the grid. In this case, the conventional VCC needs the synchronization time due to the slow dynamics of the PLL. However, the proposed method does not need synchronization process and enables to plug-and-play. From Fig 4(b) and (c), the conventional VCC tracks its references well. However, due to the slow dynamics of the PLL, the real and reactive powers have a larger oscillations and slower settling time than the proposed method, as shown in Fig 4(d) and (e). Moreover, the bandwidth of the PLL could be increased in order to obtain a better performance, as shown in Fig. 4(d) and (e). However, it is still slower than the proposed method, and the larger bandwidth of the PLL system may cause an unstable phenomenon in a weak grid [29]. Hence, we cannot increase the bandwidth of the PLL system too much. Consequently, we can conclude that the proposed method has a similar performance to the conventional VCC without using the PLL and Park transformation, but will have a better performance in some cases where the slow dynamics of PLL makes the problems.

V. EXPERIMENTAL RESULTS

The effectiveness of the proposed method is also validated by using a three-leg three-phase 15-kW inverter system with an

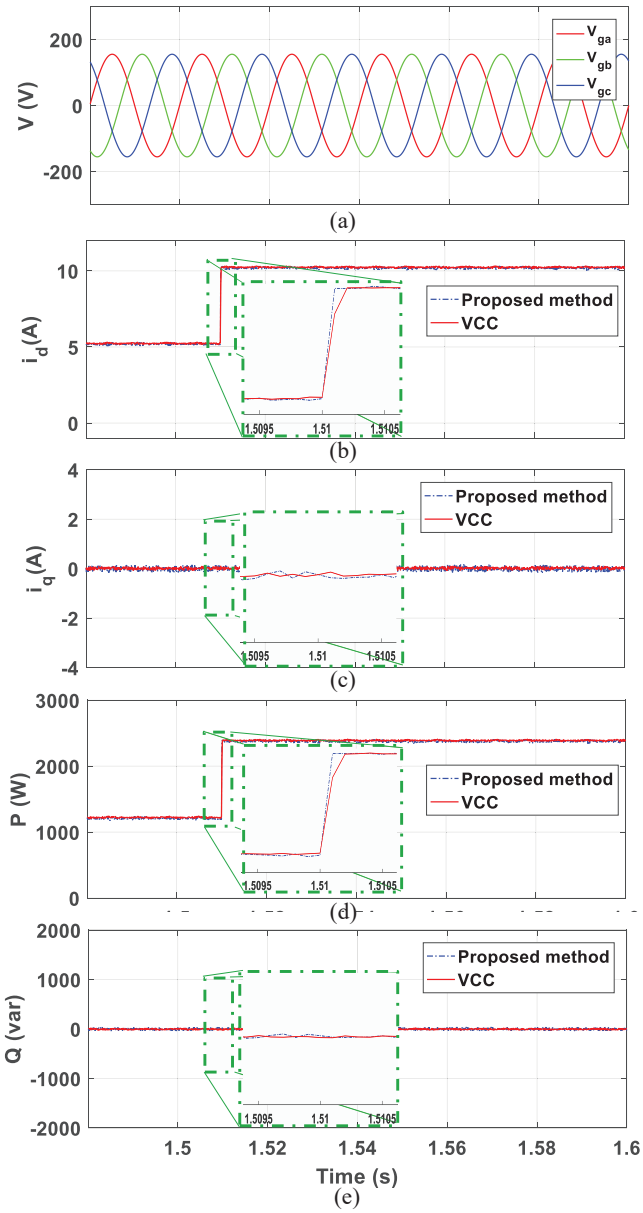

Fig. 3. Performance of the inverter when the reference of i_d is changed from 5 A to 10 A at 1.51 s. (a) grid voltage, (b) i_d, (c) i_q. (red-solid line: conventional method; blue-dashed line: proposed method).

L filter, as shown in Fig. 5(a). The controller is implemented in the DS1007 dSPACE system, where the switching pulses are generated via the DS5101 digital waveform output board, and the grid voltages and the output currents are measured through the DS2004 A/D board. The sampling and switching frequencies are set as 10 kHz. A constant DC voltage supply is used at the DC-link, and a grid simulator is connected to support 110 V RMS grid voltage at the AC side, as shown in Fig. 5(b).

A. Tracking performance

Fig. 6 shows the time response of the conventional VCC method and the proposed method when the reference of i_d is changed from 5 A to 10 A. In the experiment, the settling time

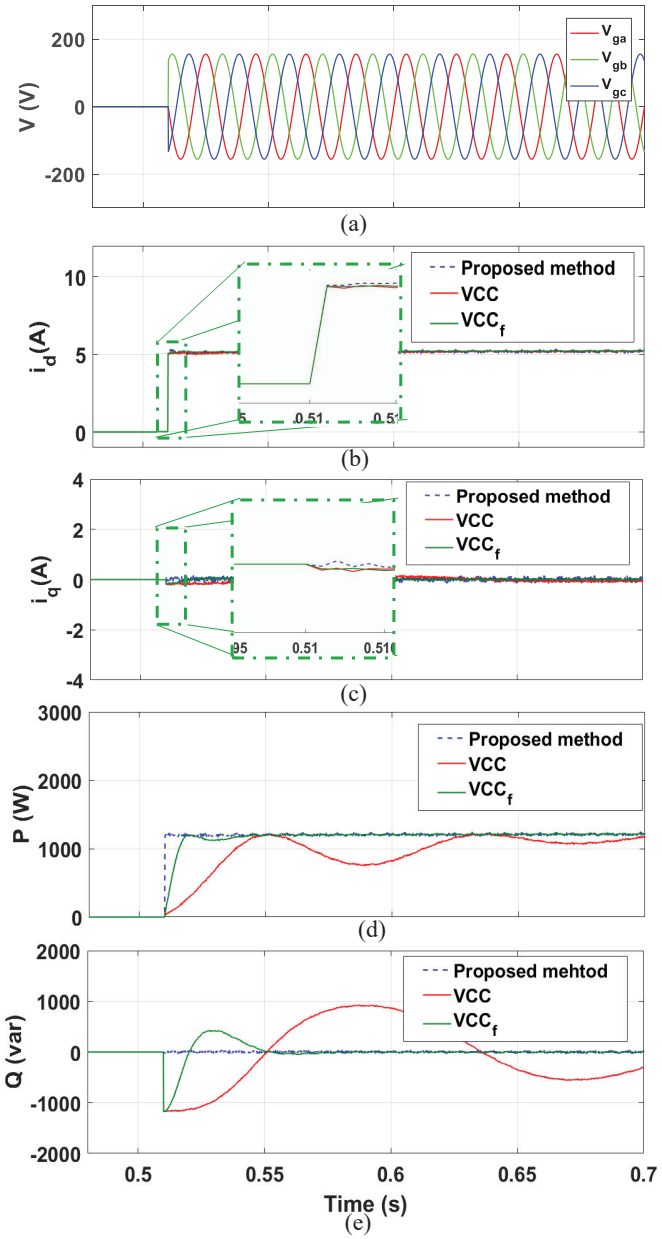

Fig. 4. Performance of the inverter when the inverter is connected at $0.51\ s$ and the reference of i_d is changed to $5\ A$. (a) grid voltage, (b) real power, (c) reactive power, (d) i_d, (e) i_q, (red-solid line: conventional VCC method; green-solid line: conventional VCC method with faster PLL; blue-dashed line: proposed method)

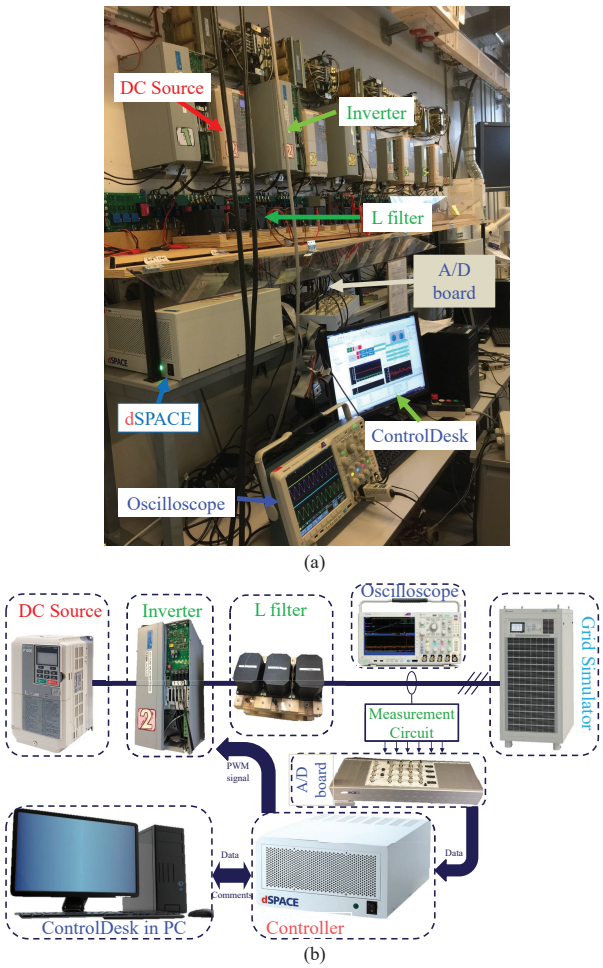

Fig. 5. (a) Photo of the experimental setup in the laboratory; (b) Configuration of experimental setup.

of the PLL system is $0.05\ s$. The blue line is the grid voltage V_{ga}, the sky-blue line is the output current I_a, and the green line is the real power P. From Fig. 6(a), the conventional VCC method has a small overshoot in the current when the reference is changed, and in the real power as well. The proposed method has a better tracking performance than the conventional VCC method, as shown in Fig. 6(b).

Fig. 7 shows the time response of both methods when the slow dynamics of the PLL affects the performance. In this case, at first, the PLL does not extract the phase angle, and then it starts estimating the phase angle when the grid voltage could be measured. The conventional VCC method has a slower settling time than the proposed method which is not using the PLL. We can conclude that the proposed method has much better performance than the conventional VCC method in the case where the PLL makes a problem.

In addition, Fig. 8 shows the time response of both methods when the reference of i_q is changed from $-5\ A$ to $5\ A$. We can observe that the proposed method has a similar performance as the conventional VCC method. Thus, we can conclude that the proposed method without the PLL and Park transformation also has a good reactive power tracking performance as well.

B. *Robustness performance*

We test also the FRT performance when the grid voltage has a voltage sag. Fig. 9 shows the time response of both methods when the grid voltage has a 25% sag. It is observed that the proposed method has a similar performance in comparison with the conventional VCC method, since the PLL does not lose the angular information in this case. We can expect that the FRT scheme could be applied to the proposed method easily.

In addition, we also test a disturbance to the variation of the frequency of the grid voltage. To compare the performance efficiently, we test a severe case where the frequency of the

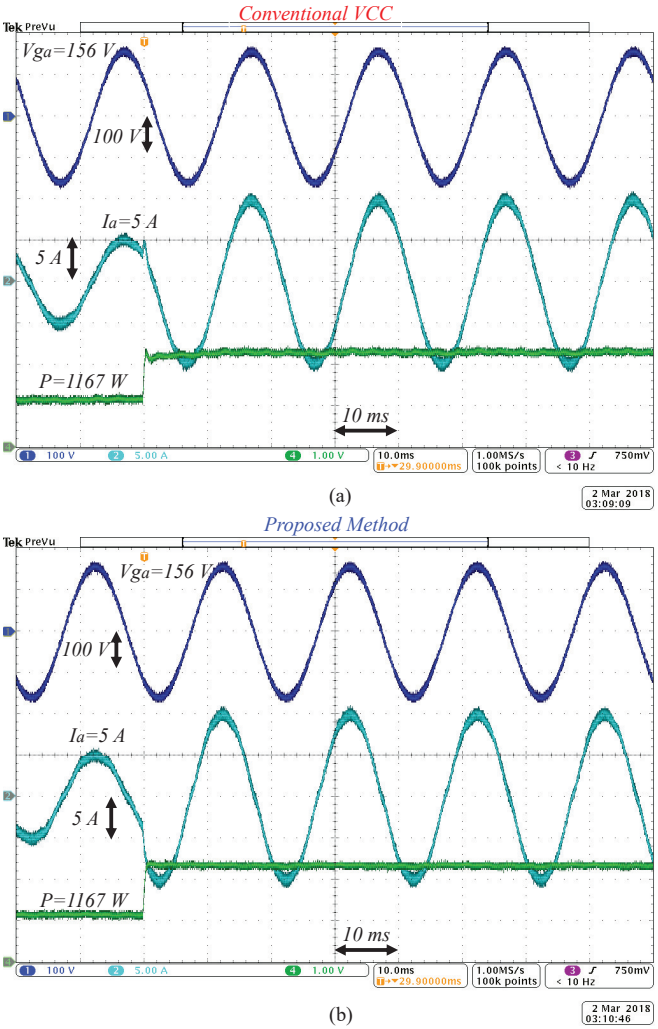

Fig. 6. Measured time response of the inverter when the reference of i_d is changed from 5 to 10 A, (a) conventional VCC method; (b) proposed method. (Blue line: grid voltage V_{ga}; Sky-blue line: output correct I_a; Green line: output power P.)

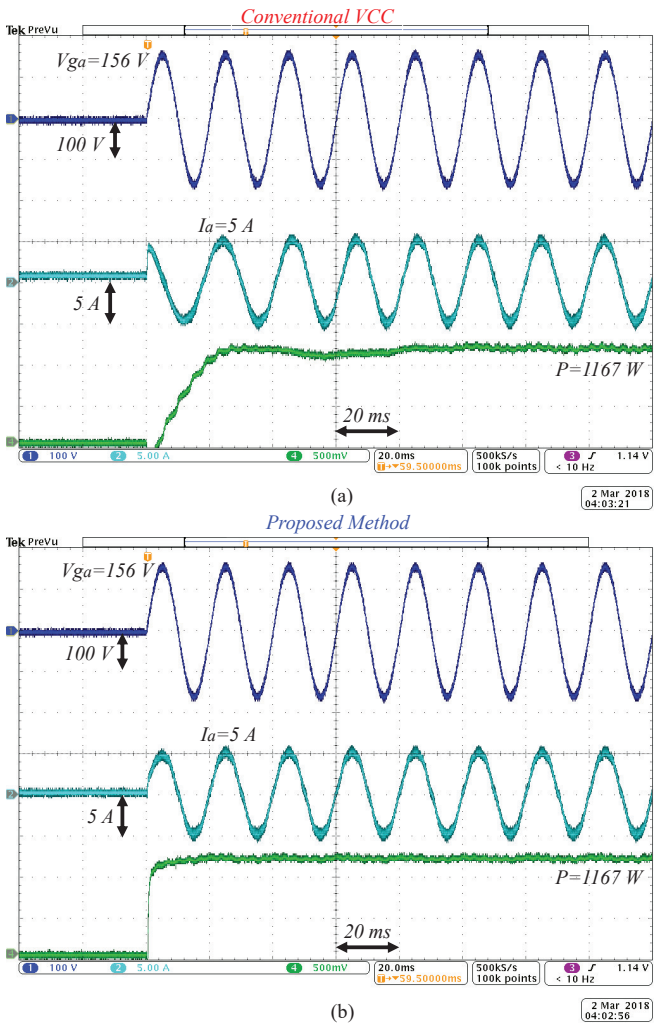

Fig. 7. Measured time response of the inverter when the inverter is connected and the reference of i_d is changed to 5 A, (a) conventional VCC method; (b) proposed method. (Blue line: grid voltage V_{ga}; Sky-blue line: output correct I_a; Green line: output power P.)

grid voltage is step changed from 48 to 52 Hz by using the grid simulator. From Fig. 10(a), the frequency of the current using the conventional VCC method cannot track the frequency fast enough when the frequency of the grid voltage is changed due to the slow dynamics of the PLL. However, Fig. 10(b) shows that the frequency of the current using the proposed method tracks the frequency of the grid voltage in one cycle, since the proposed method does not include the PLL. Consequently, we can conclude that the proposed method has robustness properties to the grid frequency variation.

Finally, to test the robustness property of the proposed method to parameter uncertainty, its performance is evaluated in the presence of the inductance variation of the filter in the control implementation. Fig. 11(a) shows the time response of the proposed method when the parameter is set to 50% of actual value in the implementation, and Fig. 11(b) shows the time response when the parameter set to 150% of actual value. To compare with Fig. 6(b), the proposed method does not lose tracking performance. Consequently, we can conclude that the proposed method has robustness properties. Moreover, we can expect that the various controllers designed based on the conventional VCC method could be applied to the proposed technique.

C. Steady-state performance

In addition, we test the case when the grid voltage has some background harmonics. At first, when the grid voltage has no harmonics, the total harmonic distortion (THD) of the current is calculated as 1.21% when the inverter regulates $i_d = 10$ A and $i_q = 5$ A, as shown in Fig. 12. Then, we inject 5^{th} and 7^{th} harmonics to the grid voltage through the grid simulator, and the THD of the grid voltage changes to 3.29%, as shown in Fig. 13(b). The performance of the inverter with the proposed method is slightly affected by these harmonics, and the THD of the current slightly increases to 3.32%, as shown in Fig. 13. However, it is still less than 5%. Moreover, we can expect that the controller designed to compensate harmonics in the d-q frame could be applied to this concept in order to solve the harmonics issues. Hence, we will modify the proposed

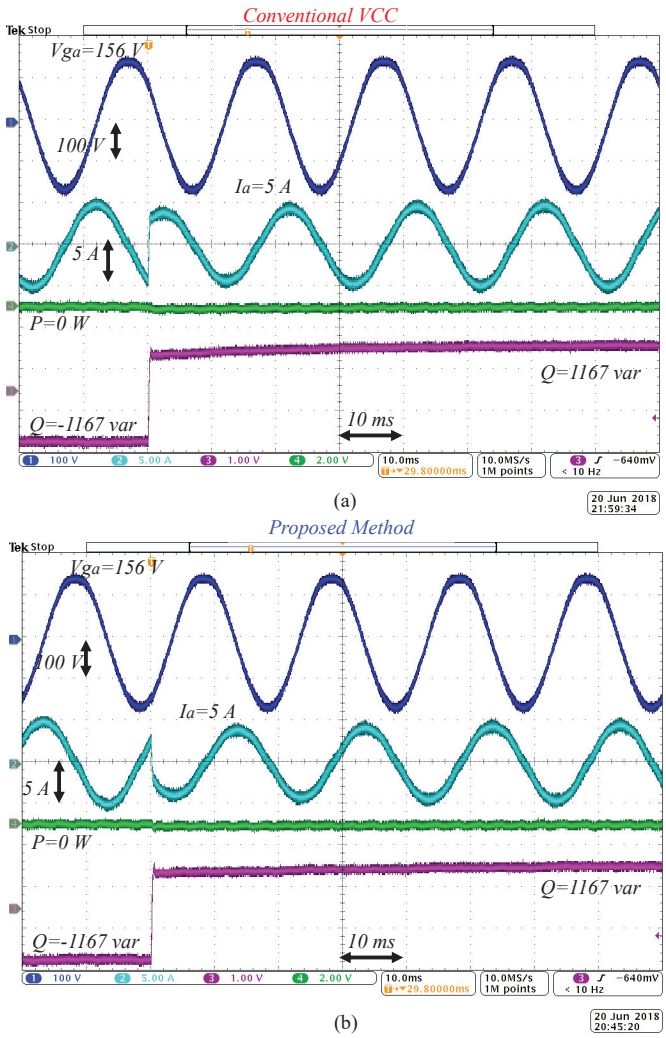

Fig. 8. Measured time response of the inverter when the reference of i_q is changed from -5 to 5 A, (a) conventional VCC method; (b) proposed method. (Blue line: grid voltage V_{ga}; Sky-blue line: output correct I_a; Green line: real power P; Purple line: reactive power Q.)

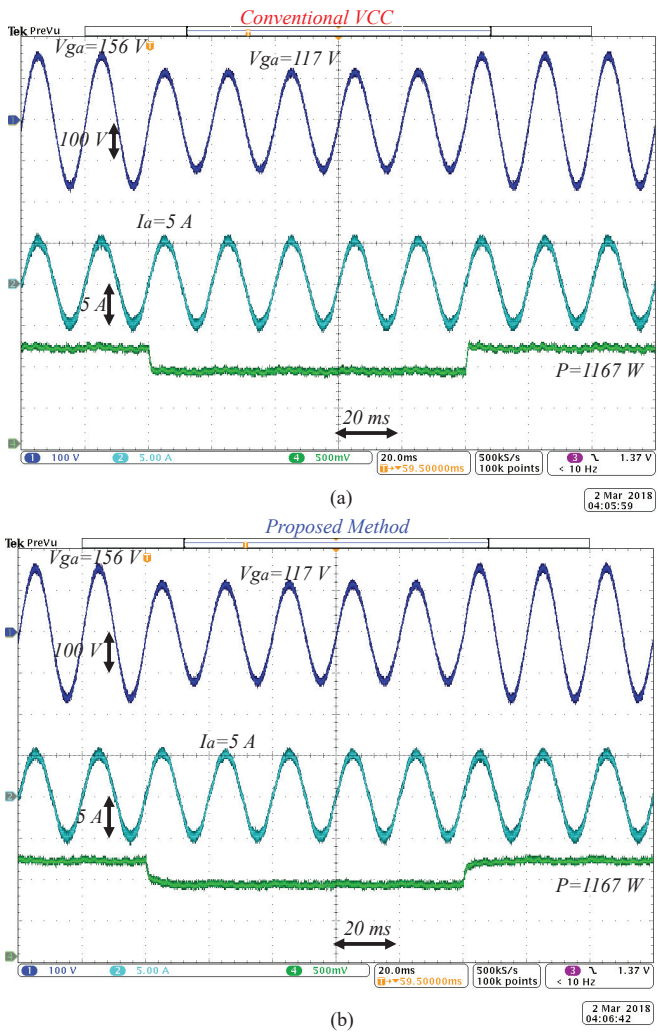

Fig. 9. Measured time response of the inverter when the grid has 25% voltage sag, (a) conventional VCC method; (b) proposed method. (Blue line: grid voltage V_{ga}; Sky-blue line: output correct I_a; Green line: output power P.)

control strategy to compensate the harmonics issues in the future. Moreover, it can be expected that the proposed method could overcome unbalanced grid voltage based on the strategy discussed in [57].

D. Weak grid test

Finally, we test the case when the inverter is connected to a weak grid (SCR=1.5), which consists of 22 mH–L and 15 μF–C impedance and a grid simulator generating 110 V RMS grid voltage. At first, the inverter injects 5 A, then. the reference is increased to 15 A. In this case, the conventional VCC method has harmonics instability phenomenon when the settling time of the PLL system is set as 0.05 s, as shown in Fig. 14(a). Wang and Blaabjerg also discussed such phenomenon in [29]. To avoid that phenomenon, we can decrease the bandwidth of the PLL as well. However, the proposed method can stabilize the system, as shown in Figure 14(b). In this case of weak grid condition, we add a band-pass filter to the voltage measurement in order to overcome the harmonic stability problem, where the fundamental component of voltage is considered. In the future, we will discuss and analyze the stability and performance of the proposed method with the band-pass filter in detail.

VI. Conclusions

In this paper, we have introduced a VCC-DPC for three-phase VSI with instantaneous real and reactive powers. We obtained the d–q axes currents model of VSI without using Park transformation and the PLL. For fair comparison, we designed a PI controller with feedforward. Thus, the proposed method has the same control structure as the conventional VCC except for the coordinate transformation and PLL. Moreover, the proposed VCC-DPC will reduce the computational burden since there is no Park transformation and as well as the PLL. Simulation results show that the proposed method has the same properties as the conventional VCC when the PLL extracts the correct phase angle of the grid voltage. However, in the case where the slow dynamics of the PLL is activated, the proposed method has improved dynamical performance in

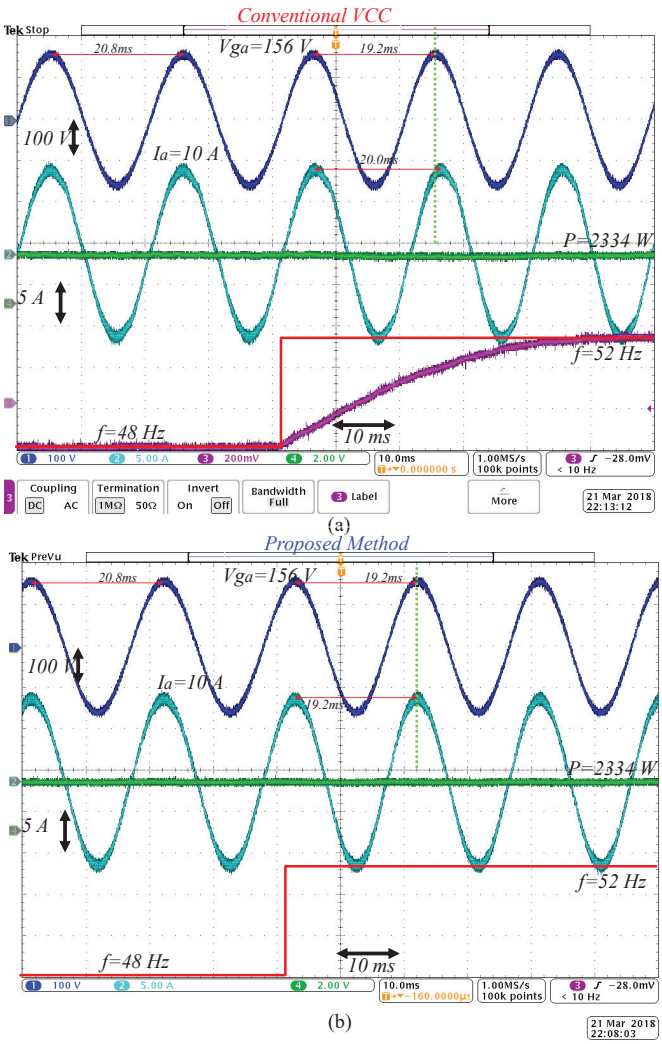

Fig. 10. Measured performance of the inverter when the grid frequency is changed from 48 to 52 Hz, (a) conventional VCC method; (b) proposed method. (Blue line: grid voltage V_{ga}; Sky-blue line: output correct I_a; Green line: output power P; Purple line: estimated frequency of the grid from PLL; Red line: frequency reference)

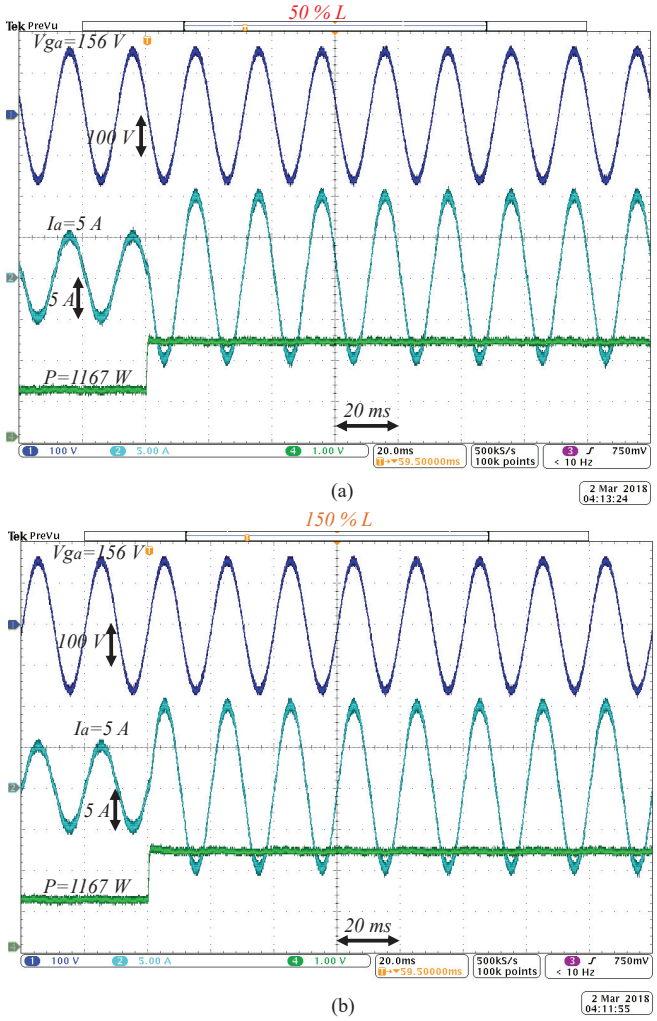

Fig. 11. Measured time response of the inverter when the inductance has some mismatch in the controller implementation, (a) 50% of L; (b) 150% of L. (Blue line: grid voltage V_{ga}; Sky-blue line: output correct I_a; Green line: output power P.)

comparison with the conventional VCC. We have also tested the performance of the proposed method with a 15-kW inverter system. Experimental results show that the proposed method has a robust property for the parameter uncertainness as well.

This work is an initial start for the VCC-DPC through the DPC model. In the future, we will design a compensator for the harmonics or unbalanced issues based on this concept.

REFERENCES

[1] F. Blaabjerg, R. Teodorescu, M. Liserre, and A. V. Timbus, "Overview of control and grid synchronization for distributed power generation systems," *IEEE Trans. Ind. Electron.*, vol. 53, no. 5, pp. 1398–1409, 2006.

[2] F. Blaabjerg, M. Liserre, and K. Ma, "Power electronics converters for wind turbine systems," *IEEE Trans. Ind. Appl.*, vol. 48, no. 2, pp. 708–719, 2012.

[3] F. Blaabjerg, Y. Yang, D. Yang, and X. Wang, "Distributed power-generation systems and protection," *Proc. IEEE*, vol. 105, no. 7, pp. 1311–1331, 2017.

[4] Q.-C. Zhong, "Power-electronics-enabled autonomous power systems: Architecture and technical routes," *IEEE Trans. Ind. Electron.*, vol. 64, no. 7, pp. 5907–5918, 2017.

[5] X. Wang, F. Blaabjerg, M. Liserre, Z. Chen, J. He, and Y. Li, "An active damper for stabilizing power-electronics-based AC systems," *IEEE Trans. Power Electron.*, vol. 29, no. 7, pp. 3318–3329, 2014.

[6] J. He, Y. W. Li, F. Blaabjerg, and X. Wang, "Active harmonic filtering using current-controlled, grid-connected DG units with closed-loop power control," *IEEE Trans. Power Electron.*, vol. 29, no. 2, pp. 642–653, 2014.

[7] X. Wang, Y. W. Li, F. Blaabjerg, and P. C. Loh, "Virtual-impedance-based control for voltage-source and current-source converters," *IEEE Trans. Power Electron.*, vol. 30, no. 12, pp. 7019–7037, 2015.

[8] L. Harnefors, X. Wang, A. G. Yepes, and F. Blaabjerg, "Passivity-based stability assessment of grid-connected VSCs–An overview," *IEEE J. Emerg. Sel. Topics Power Electron.*, vol. 4, no. 1, pp. 116–125, 2016.

[9] X. Guo, B. Wei, T. Zhu, Z. Lu, L. Tan, X. Sun, and C. Zhang, "Leakage current suppression of three-phase flying capacitor PV inverter with new carrier modulation and logic function," *IEEE Trans. Power Electron.*, vol. 33, no. 3, pp. 2127–2135, 2018.

[10] B. Wei, Y. Gui, A. Marzabal, Trujillo, J. M. Guerrero, and J. C. Vasquez, "Distributed average secondary control for modular UPS systems based microgridss," *IEEE Trans. Power Electron.*, 2018, in press, doi:10.1109/TPEL.2018.2873793.

[11] M. Kazmierkowski and L. Malesani, "Current control techniques for three-phase voltage-source PWM converters: a survey," *IEEE Trans. Ind.*

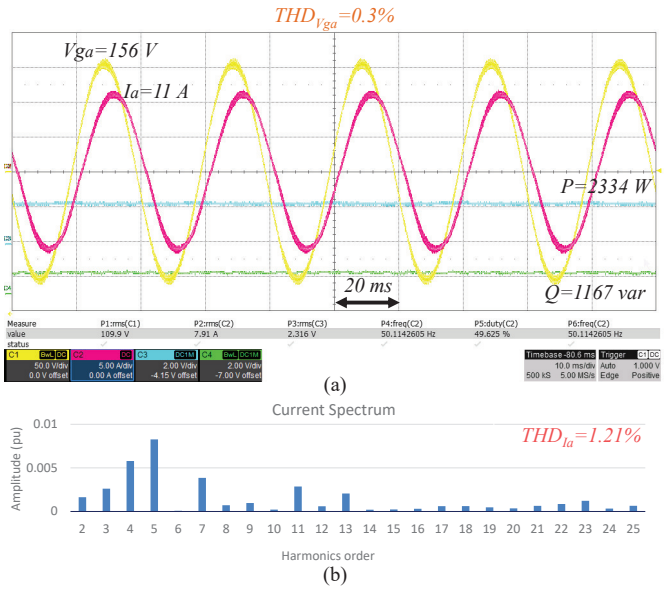

Fig. 12. (a) Measured performance of the inverter when the grid voltage has 0.3% THD during $i_d = 10\ A$ and $i_q = 5\ A$; (b) Current spectrum analysis (THD=1.21%). (Yellow line: grid voltage V_{ga}; Pink-red line: output current I_a; Sky-blue line: output real power P; Green line: reactive power Q.)

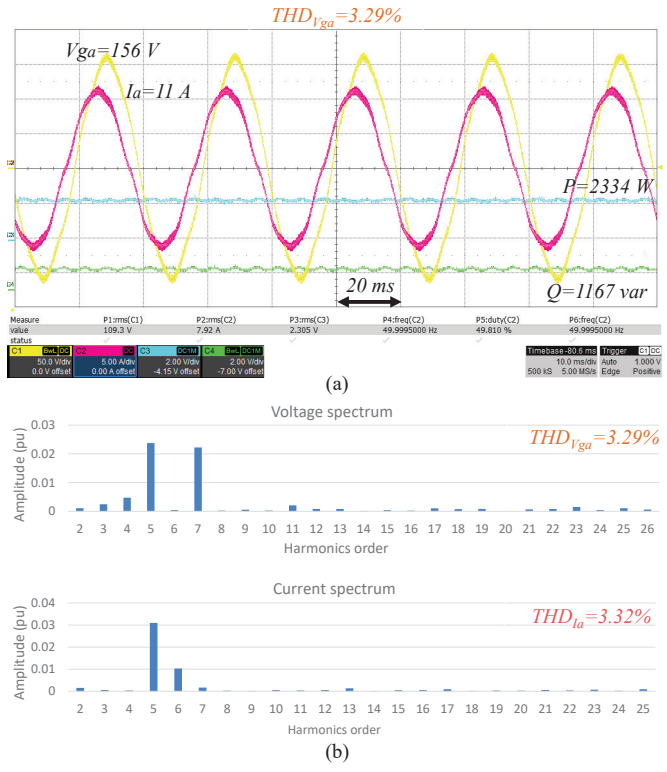

Fig. 13. (a) Measured performance of the inverter when the grid voltage has 5^{th} and 7^{th} harmonics during $i_d = 10\ A$ and $i_q = 5\ A$; (b) Spectrum analysis of voltage (3.29%) and current (THD=3.32%). (Yellow line: grid voltage V_{ga}; Pink-red line: output current I_a; Sky-blue line: output real power P; Green line: reactive power Q.)

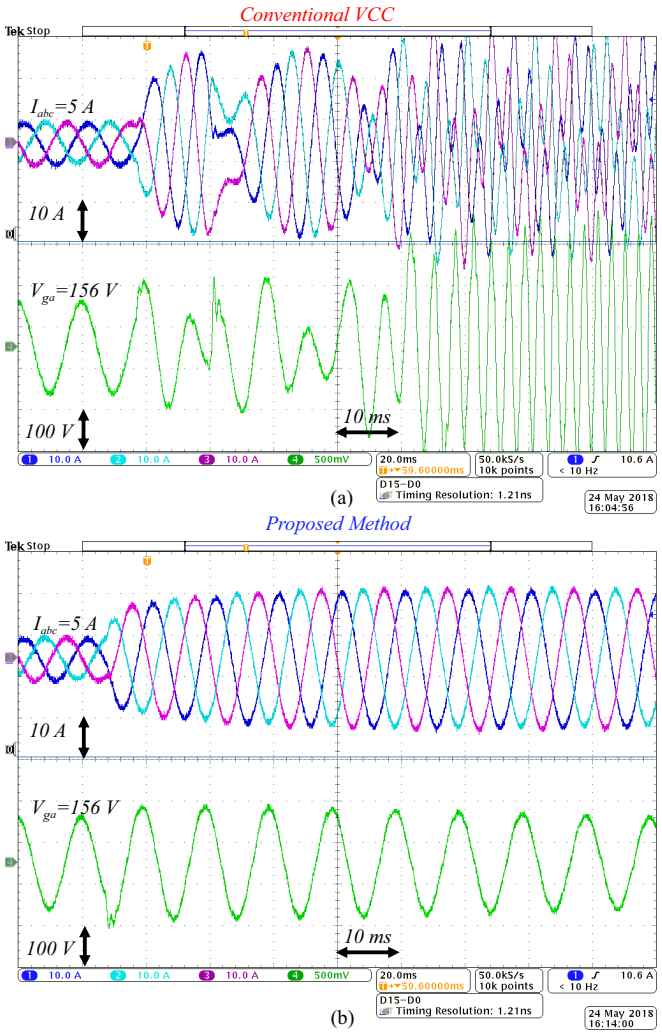

Fig. 14. Measured time response of the inverter when the reference of i d current is changed from 5 to 15 A. (a) Conventional VCC method; (b) proposed method.

Electron., vol. 45, no. 5, pp. 691–703, Oct. 1998.

[12] M. P. Kaźmierkowski, R. Krishnan, and F. Blaabjerg, *Control in power electronics: selected problems*. Academic press, 2002.

[13] E. Twining and D. G. Holmes, "Grid current regulation of a three-phase voltage source inverter with an LCL input filter," *IEEE Trans. Power Electron*, vol. 18, no. 3, pp. 888–895, 2003.

[14] R. Teodorescu and F. Blaabjerg, "Flexible control of small wind turbines with grid failure detection operating in stand-alone and grid-connected mode," *IEEE Trans. Power Electron.*, vol. 19, no. 5, pp. 1323–1332, 2004.

[15] M. Reyes, P. Rodriguez, S. Vazquez, A. Luna, R. Teodorescu, and J. M. Carrasco, "Enhanced decoupled double synchronous reference frame current controller for unbalanced grid-voltage conditions," *IEEE Trans. Power Electron.*, vol. 27, no. 9, pp. 3934–3943, 2012.

[16] B. Wen, D. Boroyevich, R. Burgos, P. Mattavelli, and Z. Shen, "Analysis of DQ small-signal impedance of grid-tied inverters," *IEEE Trans. Power Electron.*, vol. 31, no. 1, pp. 675–687, 2016.

[17] Z. Li, C. Zang, P. Zeng, H. Yu, S. Li, and J. Bian, "Control of a grid-forming inverter based on sliding-mode and mixed H_2/H_∞ control," *IEEE Trans. Ind. Electron.*, vol. 64, no. 5, pp. 3862–3872, 2017.

[18] S. Sang, N. Gao, X. Cai, and R. Li, "A novel power-voltage control strategy for the grid-tied inverter to raise the rated power injection level in a weak grid," *IEEE J. Emerg. Sel. Topics Power Electron.*, vol. 6, no. 1, pp. 219–232, 2018.

[19] V. Soares, P. Verdelho, and G. D. Marques, "An instantaneous active and reactive current component method for active filters," *IEEE Trans. Power Electron.*, vol. 15, no. 4, pp. 660–669, 2000.

[20] J. Svensson, "Synchronisation methods for grid-connected voltage source converters," *IEE Proc.-Gener., Transm. Distrib.*, vol. 148, no. 3, pp. 229–235, 2001.
[21] S.-J. Lee, H. Kim, S.-K. Sul, and F. Blaabjerg, "A novel control algorithm for static series compensators by use of PQR instantaneous power theory," *IEEE Trans. Power Electron.*, vol. 19, no. 3, pp. 814–827, 2004.
[22] G.-C. Hsieh and J. C. Hung, "Phase-locked loop techniques. A survey," *IEEE Trans. Ind. Electron.*, vol. 43, no. 6, pp. 609–615, 1996.
[23] Z. Ali, N. Christofides, L. Hadjidemetriou, E. Kyriakides, Y. Yang, and F. Blaabjerg, "Three-phase phase-locked loop synchronization algorithms for grid-connected renewable energy systems: A review," *Renew. Sustain. Energy Rev.,*, vol. 90, pp. 434–452, 2018.
[24] P. Rodríguez, A. Luna, I. Candela, R. Mujal, R. Teodorescu, and F. Blaabjerg, "Multiresonant frequency-locked loop for grid synchronization of power converters under distorted grid conditions," *IEEE Trans. Ind. Electron*, vol. 58, no. 1, pp. 127–138, 2011.
[25] M. K. Ghartemani, S. A. Khajehoddin, P. K. Jain, and A. Bakhshai, "Problems of startup and phase jumps in PLL systems," *IEEE Trans. Power Electron*, vol. 27, no. 4, pp. 1830–1838, 2012.
[26] D. Dong, B. Wen, D. Boroyevich, P. Mattavelli, and Y. Xue, "Analysis of phase-locked loop low-frequency stability in three-phase grid-connected power converters considering impedance interactions," *IEEE Trans. Ind. Electron.*, vol. 62, no. 1, pp. 310–321, 2015.
[27] M. Davari and Y. A.-R. I. Mohamed, "Robust vector control of a very weak-grid-connected voltage-source converter considering the phase-locked loop dynamics," *IEEE Trans. Power Electron.*, vol. 32, no. 2, pp. 977–994, 2017.
[28] X. Wang, L. Harnefors, and F. Blaabjerg, "Unified impedance model of grid-connected voltage-source converters," *IEEE Trans. Power Electron.*, vol. 33, no. 2, pp. 1775–1787, 2018.
[29] X. Wang and F. Blaabjerg, "Harmonic stability in power electronic based power systems: Concept, modeling, and analysis," *IEEE Trans. Smart Grid*, 2018, in press, DOI: 10.1109/TSG.2018.2812712.
[30] L. Chen, H. Nian, B. Lou, and H. Huang, "Improved control strategy of grid connected inverter without phase locked loop on pcc voltage disturbance," in *IEEE Energy Convers. Cong. Expo. (ECCE)*, 2017, pp. 4244–4251.
[31] T. Noguchi, H. Tomiki, S. Kondo, and I. Takahashi, "Direct power control of PWM converter without power-source voltage sensors," *IEEE Trans. Ind. Appl.*, vol. 34, no. 3, pp. 473–479, 1998.
[32] M. Malinowski, M. Jasiński, and M. P. Kazmierkowski, "Simple direct power control of three-phase PWM rectifier using space-vector modulation (DPC-SVM)," *IEEE Trans. Ind. Electron.*, vol. 51, no. 2, pp. 447–454, 2004.
[33] A. Bouafia, J.-P. Gaubert, and F. Krim, "Predictive direct power control of three-phase pulsewidth modulation (PWM) rectifier using space-vector modulation (SVM)," *IEEE Trans. Power Electron.*, vol. 25, no. 1, pp. 228–236, 2010.
[34] D. Zhi and L. Xu, "Direct power control of DFIG with constant switching frequency and improved transient performance," *IEEE Trans. Energy Convers.*, vol. 22, no. 1, pp. 110–118, 2007.
[35] S. Vazquez, J. A. Sanchez, J. M. Carrasco, J. I. Leon, and E. Galvan, "A model-based direct power control for three-phase power converters," *IEEE Trans. Ind. Electron.*, vol. 55, no. 4, pp. 1647–1657, 2008.
[36] J. Hu, L. Shang, Y. He, and Z. Zhu, "Direct active and reactive power regulation of grid-connected DC/AC converters using sliding mode control approach," *IEEE Trans. Power Electron.*, vol. 26, no. 1, pp. 210–222, 2011.
[37] Y. Gui, G. H. Lee, C. Kim, and C. C. Chung, "Direct power control of grid connected voltage source inverters using port-controlled Hamiltonian system," *Int. J. Control Autom. Syst.*, vol. 15, no. 5, pp. 2053–2062, 2017.
[38] S. Larrinaga, M. Vidal, E. Oyarbide, and J. Apraiz, "Predictive control strategy for DC/AC converters based on direct power control," *IEEE Trans. Ind. Electron.*, vol. 54, no. 3, pp. 1261–1271, 2007.
[39] P. Antoniewicz and M. P. Kazmierkowski, "Virtual-flux-based predictive direct power control of AC/DC converters with online inductance estimation," *IEEE Trans. Ind. Electron.*, vol. 55, no. 12, pp. 4381–4390, 2008.
[40] Z. Song, W. Chen, and C. Xia, "Predictive direct power control for three-phase grid-connected converters without sector information and voltage vector selection," *IEEE Trans. Power Electron.*, vol. 29, no. 10, pp. 5518–5531, 2014.
[41] D.-K. Choi and K.-B. Lee, "Dynamic performance improvement of AC/DC converter using model predictive direct power control with finite control set," *IEEE Trans. Ind. Electron.*, vol. 62, no. 2, pp. 757–767, 2015.
[42] J. Hu, "Improved dead-beat predictive DPC strategy of grid-connected DC–AC converters with switching loss minimization and delay compensations," *IEEE Trans. Ind. Informat.*, vol. 9, no. 2, pp. 728–738, 2013.
[43] S. Vazquez, A. Marquez, R. Aguilera, D. Quevedo, J. I. Leon, and L. G. Franquelo, "Predictive optimal switching sequence direct power control for grid-connected power converters," *IEEE Trans. Ind. Electron.*, vol. 62, no. 4, pp. 2010–2020, 2015.
[44] P. Cheng and H. Nian, "Direct power control of voltage source inverter in a virtual synchronous reference frame during frequency variation and network unbalance," *IET Power Electron.*, vol. 9, no. 3, pp. 502–511, 2016.
[45] L. Li, H. Nian, L. Ding, and B. Zhou, "Direct power control of DFIG system without phase-locked loop under unbalanced and harmonically distorted voltage," *IEEE Trans. Energy Convers.*, vol. 33, no. 1, pp. 395–405, 2018.
[46] H. Nian and L. Li, "Direct power control of doubly fed induction generator without phase-locked loop under harmonically distorted voltage conditions," *IEEE Trans. Power Electron.*, vol. 33, no. 7, pp. 5836–5846, 2018.
[47] Y. Gui, C. Kim, and C. C. Chung, "Grid voltage modulated direct power control for grid connected voltage source inverters," in *Amer. Control Conf.*, 2017, pp. 2078–2084.
[48] Y. Gui, C. Kim, C. C. Chung, J. M. Guerrero, Y. Guan, and J. C. Vasquez, "Improved direct power control for grid-connected voltage source converters," *IEEE Trans. Ind. Electron.*, vol. 65, no. 10, Oct. 2018.
[49] Y. Gui, B. Wei, M. Li, J. M. Guerrero, and J. C. Vasquez, "Passivity-based coordinated control for islanded AC microgrid," *Appl. Energy*, vol. 229, pp. 551–561, 2018.
[50] Y. Gui, M. Li, J. Lu, S. Golestan, J. M. Guerrero, and J. C. Vasquez, "A voltage modulated DPC approach for three-phase PWM rectifier," *IEEE Trans. Ind. Electron.*, vol. 65, no. 10, pp. 7612–7619, Oct. 2018.
[51] H. Kim and H. Akagi, "The instantaneous power theory on the rotating pqr reference frames," in *Proc. IEEE 1999 Int. Conf. Power Electron. Drive Syst., Hong Kong,* 1999, pp. 422-427 vol.1.
[52] H. Kim, F. Blaabjerg, and B. Bak-Jensen, "Spectral analysis of instantaneous powers in single-phase and three-phase systems with use of pqr theory," *IEEE Trans. Power Electron.*, vol. 17, no. 5, pp. 711–720, 2002.
[53] L. Harnefors, M. Bongiorno, and S. Lundberg, "Input-admittance calculation and shaping for controlled voltage-source converters," *IEEE Trans. Ind. Electron.*, vol. 54, no. 6, pp. 3323–3334, 2007.
[54] B. Wen, D. Dong, D. Boroyevich, R. Burgos, P. Mattavelli, and Z. Shen, "Impedance-based analysis of grid-synchronization stability for three-phase paralleled converters," *IEEE Trans. Power Electron.*, vol. 31, no. 1, pp. 26–38, 2016.
[55] H. Akagi, E. H. Watanabe, and M. Aredes, *The instantaneous power theory*. Wiley Online Library, 2007.
[56] F. Z. Peng and J.-S. Lai, "Generalized instantaneous reactive power theory for three-phase power systems," *IEEE Trans. Instrum. Meas.*, vol. 45, no. 1, pp. 293–297, 1996.
[57] X. Guo, W. Liu, and Z. Lu, "Flexible power regulation and current-limited control of the grid-connected inverter under unbalanced grid voltage faults," *IEEE Trans. Ind. Electron.*, vol. 64, no. 9, pp. 7425–7432, Sep. 2017.

Yonghao Gui (S'11-M'17) was born in Shenyang, China. He received the B.S. degree in automation from Northeastern University, Shenyang, China, in 2009, and the M.S. and Ph.D. degrees in electrical engineering from Hanyang University, Seoul, South Korea, in 2012 and 2017, respectively.

From 2011 to 2017, he was a Research Assistant in the System Control Lab, Hanyang University. Since February 2017, he has been working with the Department of Energy Technology, Aalborg University, Denmark, as a Postdoctoral Researcher. His research interests include control of power electronics in power systems, the Energy Internet and Smart Grid.

Dr. Gui is a member of the IEEE Power and Energy Society, the IEEE Control System Society, the IEEE Power Electronics Society, and the IEEE Industrial Electronics Society.

Xiongfei Wang (S'10-M'13-SM'17) received the B.S. degree from Yanshan University, Qinhuangdao, China, in 2006, the M.S. degree from Harbin Institute of Technology, Harbin, China, in 2008, both in electrical engineering, and the Ph.D. degree in energy technology from Aalborg University, Aalborg, Denmark, in 2013.

Since 2009, he has been with the Department of Energy Technology, Aalborg University, where he is currently a Professor and Research Program Leader for Electronic Grid Infrastructure. His research interests include modeling and control of grid-connected converters, harmonics analysis and control, passive and active filters, stability of power electronic based power systems.

Dr. Wang serves as an Associate Editor for the IEEE TRANSACTIONS ON POWER ELECTRONICS, the IEEE TRANSACTIONS ON INDUSTRY APPLICATIONS, and the IEEE JOURNAL OF EMERGING AND SELECTED TOPICS IN POWER ELECTRONICS. In 2016, he was selected into Aalborg University Strategic Talent Management Program for the next-generation research leaders. He received four IEEE prize paper awards, the outstanding reviewer award of IEEE TRANSACTIONS ON POWER ELECTRONICS in 2017, and the IEEE PELS Richard M. Bass Outstanding Young Power Electronics Engineer Award in 2018.

Frede Blaabjerg (S'86-M'88-SM'97-F'03) was with ABB-Scandia, Randers, Denmark, from 1987 to 1988. From 1988 to 1992, he got the PhD degree in Electrical Engineering at Aalborg University in 1995. He became an Assistant Professor in 1992, an Associate Professor in 1996, and a Full Professor of power electronics and drives in 1998. From 2017 he became a Villum Investigator. He is honoris causa at University Politehnica Timisoara (UPT), Romania and Tallinn Technical University (TTU) in Estonia.

His current research interests include power electronics and its applications such as in wind turbines, PV systems, reliability, harmonics and adjustable speed drives. He has published more than 600 journal papers in the fields of power electronics and its applications. He is the co-author of four monographs and editor of ten books in power electronics and its applications.

He has received 29 IEEE Prize Paper Awards, the IEEE PELS Distinguished Service Award in 2009, the EPE-PEMC Council Award in 2010, the IEEE William E. Newell Power Electronics Award 2014 and the Villum Kann Rasmussen Research Award 2014. He was the Editor-in-Chief of the IEEE TRANSACTIONS ON POWER ELECTRONICS from 2006 to 2012. He has been Distinguished Lecturer for the IEEE Power Electronics Society from 2005 to 2007 and for the IEEE Industry Applications Society from 2010 to 2011 as well as 2017 to 2018. In 2018 he is President Elect of IEEE Power Electronics Society. He serves as Vice-President of the Danish Academy of Technical Sciences.

He is nominated in 2014, 2015, 2016 and 2017 by Thomson Reuters to be between the most 250 cited researchers in Engineering in the world.